 doi:10.20944/preprints202107.0352.v1

Incidence, Spatial Pattern and Temporal Progress of Fusarium Wilt of Bananas

Daniel W. Heck[1,#a]; Miguel Dita[2]; Emerson M. Del Ponte[1]; Eduardo S. G. Mizubuti[1*]

[1] Universidade Federal de Viçosa, Viçosa, Minas Gerais, Brazil; [2] Bioversity International, Cali, Colombia; [#a] Current address: Cornell University, Geneva, New York, United States of America.

* Corresponding author: mizubuti@ufv.br

Author Contributions

Conceptualization, Daniel Heck, Miguel Dita and Eduardo Mizubuti; Data curation, Daniel Heck; Formal analysis, Daniel Heck and Emerson Del Ponte; Investigation, Daniel Heck; Resources, Miguel Dita; Supervision, Eduardo Mizubuti; Writing – original draft, Daniel Heck, Miguel Dita, Emerson Del Ponte and Eduardo Mizubuti; Writing – review & editing, Eduardo Mizubuti.

Abstract: The effective management of Fusarium wilt of bananas (FW) depends on the knowledge of the disease dynamics in time and space. The objectives of this work were: To estimate disease intensity and impact, and to investigate the spatial and temporal dynamic of FW. Fields planted with Silk (n = 10), Pome (n = 17) or Cavendish (n = 3) banana subgroups were surveyed in Brazil, totaling 95 ha. In each field, all plants were visually assessed and diseased plants were georeferenced. The incidence of FW and the impact of the disease on yield on a regional scale were estimated. Spatial patterns were analyzed using quadrat- and distance-based methods. FW incidence ranged from 0.09 to 41.42%, being higher in Silk fields (median = 14.26%). Impacts of

 doi:10.20944/preprints202107.0352.v1

epidemics on yield ranged from 18.4 to 8,192.5 kg.ha^{-1}.year^{-1}, with a median of 935.2 kg.ha^{-1}.year^{-1}. The higher economic impact of the disease was observed on Silk cultivar with a median loss of US$ 910.5 ha^{-1}.year^{-1}. Overall, estimated losses increased on average by US$ 109.8 ha^{-1}.year^{-1} at each 1% of incidence. Aggregation of FW was detected by all analytical methods in 13 fields (1 of Cavendish, 11 of Pome and 1 of Silk). In the other 17 fields, at least one analytical method did not reject the null hypothesis of randomness. One field (5 ha), composed of six plots, was selected for spatial and temporal studies during two years with bi-monthly assessments. A sigmoidal curve represented the FW progress and the Gompertz model best fitted disease progress. The level of aggregation varied over time, and evidence of secondary infection to neighboring and distant plants were detected. FW is a widespread problem in Brazil and yield losses can be of high magnitude. Epidemiology-based management strategies can now be better established.

Keywords: *Fusarium oxysporum* f. sp. *cubense*; Panama disease; epidemiology; disease impact; loss; yield; management.

INTRODUCTION

Wilted banana plants, probably due to a fungal infection, were first observed in Australia in 1874 (Bancroft 1876). In 1890, wilted plants were investigated in Cuba where Erwin F. Smith reported the soil-borne fungus *Fusarium oxysporum* associated with symptomatic banana plants (Stover 1962). It has been suggested that more than one species of *Fusarium* may be involved with the Fusarium wilt of banana (FW), also known as Panama disease. *Fusarium oxysporum* f. sp. *cubense* (E. F. Smith) W. C. Snyder and H. N. Hansen has been traditionally reported as the causal agent of FW, but another species, *F. odoratissimum* N. Maryani, L. Lombard, Kema & Crous, was

 doi:10.20944/preprints202107.0352.v1

nominated to describe one of the lineages of *F. oxysporum* capable of causing the disease (Snyder and Hansen 1940; Ploetz 2006; Maryani et al. 2019). The taxonomy of *F. odoratissimum* is under debate (Torres-Bedoya et al. 2021) and we prefer to use the traditional and most widely accepted nomenclature for the causal agent of FW: *F. oxysporum* f.sp. *cubense* (*Foc*).

Fusarium wilt is widespread in all banana growing areas. The movement of infected planting material was responsible for the fast spread of the disease worldwide (Ploetz 2015). This practice is still common among banana farmers, mainly, but not exclusively, in subsistence systems. Despite the long history of damage by FW on banana crops, there are important knowledge gaps about basic epidemiological features of FW, such as intensity, impact, and the spatio-temporal dynamics of epidemics.

Disease spatial pattern is primarily determined by biological and ecological factors related to the pathogen life-cycle (Campbell and Benson 1994) especially those related to the distribution of the primary inoculum (Ristaino and Gumpertz 2000). Knowledge gained from the analysis of spatial patterns may help generate sound scientific hypotheses about pathogen dispersal mechanisms (Macedo et al. 2019; Gigot et al. 2017), which in turn can support mitigation strategies in the case of introduction of new variants of a pathogen into an area. Additionally, spatial analyses are useful for several purposes including the study of pathogen population dynamics (Madden 1989), design of experiments (Madden and Hughes 1995), sampling programs for disease or pathogen monitoring (Madden et al. 1996; Liu et al. 2015), assessment of crop losses in relation to disease intensity (Madden and Hughes 1995), and the development of management strategies (Ristaino and Gumpertz 2000).

Disease patterns can be the realization of the dispersal of propagules (Madden et al. 2007) and despite the epidemiological implications of the understanding of spatial dynamics to disease

Preprints (www.preprints.org) | NOT PEER-REVIEWED | Posted: 15 July 2021 doi:10.20944/preprints202107.0352.v1

management, to date, only three studies provided information on the spatial pattern of FW (Meldrum et al. 2013; Liu et al. 2015; Heck et al. 2021). Aggregated pattern of FW was detected in six banana plots (1334 m^2 each) assessed in China. The higher the disease intensity, the higher was the aggregation level (Liu et al. 2015). FW was also reported to have an aggregated pattern in banana fields in Australia, but random diseased plants could also be found in some fields (Meldrum et al. 2013). Weevil borers were allegedly involved in the spread of FW and have contributed to infect banana plants far from the primary foci (Meldrum et al. 2013). In Brazil, weevil borers were detected affecting the spatial pattern of FW (Heck et al. 2021). The disease was more aggregated in a field where the population of weevil borers was managed and kept at lower numbers than in the unmanaged field (Heck et al. 2021). Another important biological fact is the potential aerial dispersal of the pathogen (Warman and Aitken 2018). If secondary infections could occur from airborne inoculum, a lower degree of aggregation and a higher number of diseased plants scattered in the field would be expected.

Other forms of spore dispersal cannot be ruled out, such as transport by animals, water, soils, substrates, and anthropogenic factors (Dita et al. 2018). Cultural practices, such as desuckering and fertilization of asymptomatic but infected plants and sharing contaminated planting materials and tools are common practices in banana plantations and contribute to the spread of FW within and between fields. The movement of symptomless seedlings, infected fruit crowns, leaf trash through shipments, or infested soil adhered to any object used by workers may have facilitated the introduction of *Foc* tropical race 4 (TR4) from Southeast Asia to Africa or to the Middle East (Ploetz et al. 2015) and even to South America. Spatial analysis may help elucidate whether an observed pattern emerged only by chance or due to an underlying process that may or may not be known. To succeed in such endeavour it is necessary to use analytical methods based

Preprints (www.preprints.org) | NOT PEER-REVIEWED | Posted: 15 July 2021 doi:10.20944/preprints202107.0352.v1

on different approaches for inspecting spatial patterns at different scales since the impact of a pattern on a process can vary with the scale (Szmyt 2014).

Classic and current texts emphasize the potential large contribution of infected plants or contaminated tools to the spread of FW in banana fields (Stover 1972; Dita et al. 2018). By examining the pattern of FW epidemics in fields it is possible to infer that autochthonous inoculum of Foc would most likely result in random or regular distribution of wilted banana plants, whereas external inoculum from contaminated transplants or tools would result in aggregation or clusters of diseased plants. Pattern analysis and the study of spatio-temporal dynamics of epidemics can shed light on the contribution of the origin of the inoculum of FW epidemics in banana plantations. However, these studies are largely absent for the FW-banana pathosystem. The objectives of this study can be summarized by the following research questions: (i) what is the intensity and (ii) the impact of FW in different production regions and cultivars in Brazil?; (iii) what is the predominant spatial pattern of FW epidemics at different scales?; (iv) what is the temporal dynamic?; and (v) how does the spatial distribution change over time?

MATERIAL AND METHODS

Fields

Thirty banana fields with records of FW incidence were assessed from March 2016 to April 2017. The fields were grouped based on geographic location: Vale do Ribeira (VR; N = 4 fields); São José do Rio Preto and Araçatuba (SJA; N = 8), in São Paulo state; Serra da Mantiqueira and Zona da Mata (SMZM; N = 6), in São Paulo and Minas Gerais states, respectively; Norte de Minas and Vale do São Francisco da Bahia (NMSF; N = 5), in Minas Gerais and Bahia states, respectively; Norte Catarinense (NC; N = 5), in Santa Catarina state; and Norte Pioneiro

Preprints (www.preprints.org) | NOT PEER-REVIEWED | Posted: 15 July 2021 doi:10.20944/preprints202107.0352.v1

Paranaense (NPP; N = 2), in Paraná state (Fig. 1A). The fields were located within 13°14'S to 26°28'S latitude and 43°21'W to 50°50'W longitude. Altitude ranged from 45 masl in VR to 1150 masl in SMZM. These five states accounted for 43% of the planted area and 53% of the total Brazilian banana production in 2017 (IBGE 2019). Field size ranged from 0.85 to 6.67 ha and was planted with Silk (N = 10 fields; a total of 34.7 ha), Pome (N = 17; 51.4 ha) or Cavendish (N = 3; 8.5 ha) banana subgroups.

Disease intensity

In each field, all banana plants were visually assessed for typical external and internal symptoms of FW. External symptoms corresponded to plant wilting, yellowing of older leaves, the collapse of leaves at the base of the petiole, fallen and dried leaves around the pseudostem, wrinkling and distortion of leaf blades, and splitting at the base of pseudostem. Internal symptoms were observed when external symptoms were not evident, but the plant appeared infected. A small cut in the pseudostem was made to verify yellow, reddish-brown, or black discolorations in vascular tissues (Carlier et al. 2002). If external and internal symptoms were present in at least one plant of the mat, the whole mat was considered diseased and was georeferenced using a handheld GPS device (GPSMAP® 64, Garmin). When symptoms were not clearly assigned to FW, samples were collected for further confirmation using laboratory analyses. For each field, data sets containing the polygon used to delimit the field perimeter and the diseased plants' geographic coordinates were used for spatial analyses using the R software version 3.6.1 (R Core Team 2019).

The number of diseased plants (y) in each field was recorded, and the incidence ($\hat{p}$) was calculated as $\hat{p} = y / \hat{n}_i$, where $\hat{n}$is the estimated number of plants. The$\hat{n}_i$ was calculated using the polygon representing the field perimeter (used to estimate the area) and plant spacing (plant

Preprints (www.preprints.org) | NOT PEER-REVIEWED | Posted: 15 July 2021 doi:10.20944/preprints202107.0352.v1

distance within and between rows). Disease intensity was compared among regions and cultivars. The data were submitted to Shapiro-Wilk and Bartlett's tests and transformed by log(x) before analysis of variance (ANOVA). Comparisons were performed by Tukey HSD test for unbalanced data. All the following spatial and temporal statistics were calculated using disease incidence as proportion. The incidence values were presented as the percentage of infected plants.

Estimated losses

Yield loss (L) per unit area (ha) for each field was calculated based on $L = W * \hat{p}$, where W is the actual yield of the banana crop per year (ton.ha^{-1}.year^{-1}) and $\hat{p}$ is the incidence (proportion) (Madden et al. 2007). The actual yield is the average yield of the municipality in which a field was located (IBGE 2019; Table 1). Economic losses were calculated as L (US$) = $L * \bar{P}_s$, where $\bar{P}$ is the average price for each banana subgroup (s). Monthly prices from 2013 to 2016 for each banana variety were obtained from Fala.BR (https://www.gov.br/acessoainformacao/). Linear regression was used to analyze the relationships between yield loss and the disease incidence, $L = \beta_0 + \beta_1\hat{p}$, where β_0 and β_1 are regression parameters, and $\hat{p}$ is FW incidence (Madden et al. 2007). Yield losses were also compared among regions and banana subgroups. The data were submitted to Shapiro-Wilk and Bartlett's tests and transformed by log(x) before ANOVA for unbalanced data followed by Tukey HSD multiple comparison test.

Spatial pattern analyses

Analytical methods based on quadrats and on distances were used to investigate the spatial patterns at different spatial and temporal scales.

Preprints (www.preprints.org) | NOT PEER-REVIEWED | Posted: 15 July 2021 doi:10.20944/preprints202107.0352.v1

Quadrat-based methods

Incidence maps were quadratized using the *quadratcount* function of the *spatstat* package (Baddeley and Turner 2005). The exact number of plants in each quadrat could not be computed because the rows were not regularly spaced or straightly set in most fields. The maximum number of plants in a quadrat was assumed to vary from 4 in 2 x 2 to 36 in 6 x 6 quadrat-sizes. The sampling unit area varied among fields because different spacing between plants was observed, but the relationship of the distance within and between rows was the same. The number of diseased plants in each quadrat was determined and used in the spatial analysis.

Spatial hierarchy. Initially, four hierarchical levels, 2 x 2 (lowest), 3 x 3, 4 x 4, and 6 x 6 (highest) estimated plants per quadrat, were used to characterize the sampling units. Analyses of β-binomial curves were used to assess aggregation within-sampling-unit. The spatial hierarchy analysis was performed using *spatial_hier* from *epiphy* R package (Gigot 2018).

Dispersion index. The index of dispersion for binomial data, D, was calculated for each field as the ratio of the observed and the estimated variances (Madden and Hughes 1995). A χ^2 test was performed to test if the dispersion index equals 1 (D = 1). The analysis was conducted using the *agg_index* function from the *epiphy* R package.

Fitting distributions. The binomial and β-binomial distributions were fitted to the disease incidence data for each field. The χ^2 goodness-of-fit test for both distributions and a log-likelihood ratio test (LRS) was used to determine whether the β-binomial better fits the observed frequency than the binomial distribution. This analysis was performed using the *fit_two_distr* function from the *epiphy* R package.

Preprints (www.preprints.org) | NOT PEER-REVIEWED | Posted: 15 July 2021 doi:10.20944/preprints202107.0352.v1

Binary power law. The binary power law was used to evaluate the relationship between the observed variance and the corresponding variance on the assumption of a binomial distribution of FW incidence using an intermediate quadrat-size (3 x 3) (Madden et al., 2007). Categorical values referring to the different banana subgroups, Cavendish, Pome, or Silk, were included in data sets. A modified t-test compared the model's parameter estimates against the null hypothesis and between them.

Distance-based methods

Spatial Analysis by Distance IndicEs (*SADIE*). This method uses the location of the sampling units (quadrats) and the number of diseased individuals inside the unit to analyze the spatial arrangement of the diseased individuals by the distance to regularity (D_r) (Perry et al. 1999). The modified index developed by Li et al. (2012) was computed by the *sadie* function from *epiphy* R package.

Events and intervals. The distance-based statistic (Madden et al. 2007) was used as an alternative to quadrat-based methods. In this analysis, patterns of points were described based on intervals in space among events. The goodness-of-fit of the point process model was performed using a *cdf.test* function from *spatstat* package.

L(*d*) *function*. Ripley's *K*(*d*) function is a cumulative distribution function useful to analyze completely mapped spatial point process data (Dixon 2014). *K*(*d*) considers the entire distribution of distances rather than just the mean of neighbor events (Dixon 2014; Madden et al. 2007). *L*(*d*) is a transformed version of *K*(*d*), on which the expected *K* value is equal to distance (Besag 1977). The analyses were performed using *Lest*, *envelope*, and *mad.test* functions from *spatstat* R package.

Preprints (www.preprints.org) | NOT PEER-REVIEWED | Posted: 15 July 2021 doi:10.20944/preprints202107.0352.v1

Semivariance. The semivariance (γ) is a measurement of one-half of the variance between values separated by the same distance in a specific direction. Samples separated at distances greater than the range may be considered spatially independent (Madden et al. 2007). The semivariance and the parameters were calculated using the *variog* and *variofit* functions from *geoR* (Ribeiro and Diggle 2018).

Concordance analyses

The statistical methods were transformed into categorical data (aggregated or random) and tested by Cohen's kappa for paired agreement among the methods and Fleiss's kappa for an overall agreement of all methods used. The analysis was performed using the *kappa2* and *kappam.fleiss* functions from the *irr* package (Gamer et al. 2019).

Temporal analysis

One Prata (Pome subgroup) banana field with 4.4 ha established in 2012 in Teixeiras, Minas Gerais state, Brazil, was selected to study the disease dynamics in space and time. The area was cultivated in a low-input system, with minimal cultural practices. Six plots delimited by dirty roads, ranging from 0.3 to 1.0 ha, were set in the field. The number of plants per plot ranged from 171 to 649. Plants were spaced approximately 3 x 5 m, within and between rows, respectively. The plots were assessed from April 2017 to February 2019 every two months, resulting in 12 disease assessments. Disease incidence was assessed as described above.

Hourly records of temperature, relative humidity, and precipitation data were obtained from the closest standard weather station located at 14.4 Km from the field. Data were provided

Preprints (www.preprints.org) | NOT PEER-REVIEWED | Posted: 15 July 2021 doi:10.20944/preprints202107.0352.v1

by Instituto Nacional de Meteorologia (INMET) of Ministério da Agricultura, Pecuária e Abastecimento (MAPA).

The cumulative incidence was calculated for each plot in different assessment times. The Monomolecular, Logistic, and Gompertz models were fit to the disease incidence and plotted over time by nonlinear regression analysis using the *nlsLM* function from the *MINPACK.LM* package (Elzhov et al. 2016). The best model was chosen based on the lower root mean square error (RMSE), independence and homogeneity of variances, and higher coefficient of determination (R^2).

Spatio-temporal dynamics

Spatio-temporal analyses were performed for the same six plots assessed in Teixeiras for temporal analyses. The index of dispersion, *SADIE*, binary power law, and spatio-temporal association analyses were used to describe the spatial pattern of the disease on the plots over time. A spatio-temporal association study assesses the significance of the correlation coefficient between two spatially autocorrelated processes (Clifford et al. 1989; Dutilleul et al. 1993). The measurement of the degree of local clustering in sampling units was used to calculate the similarity in the cluster indices of two sequential assessments. The local clustering (χ_p) was obtained by *SADIE* analysis (Li et al. 2012), and the overall association, *X*, was acquired by the correlation coefficient of the local clustering between pairs of assessments. The t-test corrected for the spatial association was used to test the significance of χ^2 distribution (Dutilleul et al. 1993). The analysis was performed using the *sadie* and *modified.ttest* functions from *epiphy* and *SpatialPack* (Osorio and Vallejos 2018) packages, respectively.

Preprints (www.preprints.org) | NOT PEER-REVIEWED | Posted: 15 July 2021 doi:10.20944/preprints202107.0352.v1

RESULTS

Disease intensity

FW incidence ranged from 0.09 to 41.4% across the fields located in different regions in Brazil (Fig. 1A). The mean and median incidence values were 10.68% and 4.98%, respectively (Fig. 2B, Table 2). The incidence varied among regions (P = 0.036). The highest average incidence was 22.13% in NPP (n = 2 fields) followed by SJA (n = 8) with an average of 17.75%. In other regions, the average incidence values were less than 9.82% (Fig. 1B).

The incidence of FW varied among cultivars (P = 0.017). The highest value of average incidence was observed for Silk (n = 10 fields), 18.62%. The widest range of incidence values was recorded on Silk fields: minimum of 4% and maximum of 41.4%. Pome fields (n = 17) had intermediate incidence values: average of 7.46%, and ranging from 0.1% to 33.4%. Lowest disease incidence were recorded on fields planted with Cavendish (n = 3) with an average of 2.43% and ranging from 1.8% to 2.8% (Fig. 1C).

Estimated losses

The yield losses in the 30 fields ranged from 18.4 to 8,192.5 Kg.ha^{-1}.year^{-1} (Fig. 2A). The mean value was 1,856.5 Kg.ha^{-1}.year^{-1} with a median of 935.2 Kg.ha^{-1}.year^{-1}. Yield losses did not vary among banana subgroups (P = 0.10). Economic losses reached a maximum of 5,244.8 US$.ha^{-1}.year^{-1}, with a mean value of 1,010.4 US$.ha^{-1}.year^{-1} and a median of 405.1 US$.ha^{-1}.year^{-1} (Fig. 2B). Differences were observed for economic losses (P = 0.01) among banana subgroups. Silk differed (P = 0.016) from the Pome subgroup with median loss of 910.6 US$.ha^{-1}.year^{-1} and 343.1 US$.ha^{-1}.year^{-1}, respectively.

Preprints (www.preprints.org) | NOT PEER-REVIEWED | Posted: 15 July 2021 doi:10.20944/preprints202107.0352.v1

A positive linear trend was detected for the relationships between FW incidence and both the estimated yield and economic losses (Fig. 2C and D). The intercept parameter of both regression models, β_{0yield} = -112.3 (SE = 250.3) and $\beta_{0US\$}$ = -162.4 (SE = 151.4), did not differ from 0 ($P > 0.29$). The slope parameter of both regression models, β_{1yield} = 184.4 (SE = 15.8) and $\beta_{1US\$}$ = 109.8 (SE = 9.53), differed from 0 ($P < 0.001$). The 95% confidence interval (CI 95%) of the slope for estimated yield losses ranged from 152.1 to 216.7 Kg.ha^{-1}.year^{-1}, and for economic losses from 90.3 to 129.4 US$.ha^{-1}.year^{-1}. The effects of banana cultivars were not significant ($P > 0.16$).

Spatial pattern analyses

Quadrat-based methods

At all four hierarchical levels the β-binomial curves fell under the binomial curves (Fig. 3). Values of v, interpreted as effective sample size, were lower than the real number of individuals (n) for all hierarchical levels ($P < 0.001$). Effective sample sizes were estimated at v_{2x2} = 2.79 (± 0.12) for the 2 x 2 quadrat-size containing 4 individuals, v_{3x3} = 5.22 (± 0.32) for quadrats of 9 individuals, v_{4x4} = 7.95 (± 0.67) for quadrats of 16 individuals, and v_{6x6} = 13.73 (± 1.48) for the 6 x 6 quadrat-size containing 36 individuals at the highest level (Fig. 3). These values of v correspond to 69.8%, 57.9%, 49.7%, and 38.2% of n in the four hierarchical levels, respectively. Only the intermediate quadrat-size (3 x 3) was used in subsequent quadrat-based analyses.

The dispersion index, D, ranged from 1 to 6.5 and the median value was 2.3 (Fig. 4A). Overall, there were no differences among regions regarding D ($P = 0.119$) and aggregation was inferred in all fields and regions, but for a single field (out of 5) in the NMSF region where a random pattern of FW was detected (Table 2).

Preprints (www.preprints.org) | NOT PEER-REVIEWED | Posted: 15 July 2021 doi:10.20944/preprints202107.0352.v1

The frequency of diseased plants in quadrats was well described for 90% of the fields by the β-binomial distribution ($P > 0.05$) (Table 2). For one field the frequency was better described by the binomial distribution (data not shown). The θ parameter of the β-binomial distribution ranged from 0.02 to 2.01 (median = 0.20) (Fig. 4B). There were no differences among regions for the θ parameter ($P = 0.26$). The distribution of diseased plants was better described by the β-binomial than by the binomial distribution in 96.7% of the fields ($P < 0.05$) (Table 2). The only case where the LRS was not significant, i.e. the binomial and β-binomial models could both describe the distribution of diseased plants, was in a 'Pome' field located in NMB where the FW incidence was very low (0.5%).

The relationship between the logarithm of the observed and theoretical variances for binomial data from 30 fields was well described by the binary power law ($R^2 = 0.955$) (Fig. 6A). The overall estimates of binary power law parameters, $\log(A_p)$ (2.09 ± 0.28) and b (1.227 ± 0.05), were significantly ($P < 0.001$) higher than 0 and 1, respectively. The disease had an aggregated pattern and the degree of aggregation was influenced by incidence. FW had an aggregated pattern in Silk and Pome fields ($P < 0.001$) (Fig. 6B). The estimated parameters from the binary power law differed for Silk and Pome ($P < 0.03$). In general, the level of aggregation was higher and more influenced by incidence in Silk ($\log(A_p) = 2.77 \pm 0.41$, $b = 1.40 \pm 0.09$) than in Pome fields ($\log(A_p) = 2.37 \pm 0.45$; $b = 1.26 \pm 0.07$). Cavendish fields did not differ from Silk and Pome for both parameters ($\log(A_p)$ and b; $P > 0.05$).

Distance-based methods

The distance to regularity (D_r) computed by SADIE was calculated for all fields. The aggregation index (I_a) ranged from 0.93 to 3.86 and the median value was 1.75 (Fig. 4C).

Preprints (www.preprints.org) | NOT PEER-REVIEWED | Posted: 15 July 2021 doi:10.20944/preprints202107.0352.v1

Differences among regions were not observed for I_a (P = 0.114). Considering the 30 fields in six regions, the random pattern of FW was inferred for 10 (33.3%) fields (Table 2). Five of them were located at SJA, all planted with Silk cultivar.

The maximum difference ($D_{K\text{-}S}$) between the observed and expected distributions ranged from 0.064 to 0.566 (median = 0.187) (Fig. 4D). The hypothesis of randomness for K-S statistic was rejected for 73.3% of the fields (Table 2). The smallest values of $D_{K\text{-}S}$ were observed in SJA and NC (mean of 0.130). In SJA and NC a random pattern of FW was inferred in almost all fields and there was no evidence to reject the null hypothesis in 50% and 60% of the fields, respectively. In the NMSF region a random pattern of FW was inferred in a single field with an intermediate value for $D_{K\text{-}S}$ (0.214) and the lowest FW incidence (0.09%).

The second-order point-pattern analysis used Ripley's K and the linearized form $L(d)$ function. The maximum absolute deviation (MAD) statistic ranged from 1.61 to 58.34 m with a median of 6.91 m (Fig. 4E). Observed values of $L(d) - d$ for 96.7% of the fields were higher than the critical values of the simulated envelope and resulted in aggregation (Fig. 5A). Only one field resulted in a random pattern (P = 0.34). This field was cultivated with 'Pome' cultivar, had a low incidence of FW (0.49%) and the random pattern was also inferred by two quadrat-based statistics (D and LRS). The distance that resulted in the highest scale of aggregation (max $L(d) - d$) for each field is shown in Fig. 5A.

Semivariance was successfully performed by the spherical model in 27 of 30 fields (Fig. 4F). Three fields (10%) had higher spatial variability at scales smaller than the distance between sampling units and the semivariance parameters could not be computed. Semivariance parameters varied with fields. Those with higher incidence had higher values of semivariance (R = 0.87; data not shown). The *nugget* parameter ranged from 0 to 4.62 with a median of 0.40 and *sill* ranged

Preprints (www.preprints.org) | NOT PEER-REVIEWED | Posted: 15 July 2021 doi:10.20944/preprints202107.0352.v1

from 0.01 to 5.06 (median of 0.46) (Fig. 5B). The observed values of the *range* parameter varied from 9.36 to 154.61 m with a median of 30.80 m (Fig. 4F and 5B).

Concordance analyses

The FW epidemics had either random or aggregated patterns. Cohen´s Kappa paired agreement was weak or non significant for most of the spatial statistics (Table 3). Two pairwise tests had a significant agreement. One was a strong agreement (1; $P < 0.001$) between the aggregation index (D) and the MAD statistic on which all fields are classified in the same category (aggregated). The second was a weak agreement of *SADIE's* aggregation index (I_a) with $D_{K\text{-}S}$ statistic (0.37; $P = 0.04$), with 22 of 30 fields presenting the same spatial pattern. Fleiss's Kappa (overall agreement) did not reject the null hypothesis for a random classification of all spatial analyses ($P = 0.63$). Agreement could not be detected by the test in 43.3% (13/30) for the fields that presented the aggregated patterns and none of them were classified as random for all spatial statistics (Table 3).

Temporal analyses

On the first assessment, the incidence ranged from 0 to 0.03 with a mean and median both of 0.01 (Fig. 7). Five of six plots already had symptomatic FW plants before the beginning of the assessments. After six assessments the incidence in all plots ranged from 0.02 to 0.09 with a median of 0.06 and in the last assessment the FW incidence ranged from 0.05 to 0.15 with a median of 0.1. The Gompertz model best fitted the disease incidence data over time in all plots (*data not shown*). The estimated parameters of the model, as the initial incidence (y_0) ranged from 0.003 to

Preprints (www.preprints.org) | NOT PEER-REVIEWED | Posted: 15 July 2021 doi:10.20944/preprints202107.0352.v1

0.028 with a median of 0.015 and the disease progress rate (*r*) from 0.096 to 0.148, with mean and median values of 0.127 and 0.135, respectively (Fig. 7).

Spatio-temporal dynamics

Among the different quadrat-based methods, the aggregation index (*D*) was chosen to assess the spatial pattern of FW at small scale. In 11 of 12 assessments, banana plants with symptoms of FW were aggregated in all six plots (Fig. 8A). In the first assessment conducted in April 2017, *D* ranged from 1.35 to 3.00 with a median value of 1.52. In the last assessment, February 2019, *D* ranged from 2.55 to 5.06 with a median of 4.18. *D* increased linearly with the FW progress ($P < 0.001$).

Among the distance-based methods, *SADIE* was the method used to characterize the heterogeneity of patches and gaps of diseased banana plants over time. The I_a differed from 1 ($P < 0.05$) in only two plots, which correspond to 33.3% of the plots analyzed (Fig. 8B). Four plots did not differ from a random pattern ($P > 0.05$). I_a did not change during the period of study ($P = 0.51$). In the first assessment, April 2017, I_a ranged from 0.78 to 1.98 with a median value of 1.01. In February 2019, I_a ranged from 0.86 to 2.21 with a median of 1.47.

The relationship between the logarithm of observed and binomial variances for six plots in bimonthly assessments was well described by the binary power law ($R^2 = 0.914$) (Fig. 8C). Overall, parameter estimates for power law, $\log(A_p) = 0.882 \pm 0.029$, and $b = 1.154 \pm 0.034$, were significantly different from 0 and 1, respectively, when all plots were jointly analyzed ($P < 0.001$). As $\log(A_p)$ was higher than 0 and *b* higher than 1, the pattern of FW was inferred to be aggregated and the degree of aggregation varied with disease incidence.

Preprints (www.preprints.org) | NOT PEER-REVIEWED | Posted: 15 July 2021 doi:10.20944/preprints202107.0352.v1

Spatio-temporal associations were detected between the pairs of successive assessments for the local clusterings ($P < 0.05$) (Fig. 8D). In the first and second assessments, April and June of 2017, three of the five plots had no association ($P > 0.07$). At this time, X values ranged from 0.41 to 0.91 with a median of 0.71. After the third association, August 2017 and October 2017, all pairwise comparisons were significantly associated for all plots ($P < 0.05$). In the last association, X ranged from 0.92 to 0.99 (Fig. 8D).

DISCUSSION

The gap of knowledge related to the spatio-temporal dynamics of FW and the lack of estimates of the economic impact of the disease have been raised in previous studies (Dita et al. 2018; Scheerer et al. 2018; Staver et al. 2020). Based on the disease distribution within fields and regions, hypotheses can be developed to understand the ways plant pathogens can be dispersed. The dynamics of the disease over time, and information of social and economic impact of a plant disease are key for implementing resources and efforts to guide strategies to manage plant diseases (Staver et al. 2020). Regarding those assumptions, this work assessed the intensity, investigated the spatial and temporal dynamics, and estimated the yield and economic impact of FW in 30 banana fields (94.6 ha) in six different production regions in Brazil. In total, 109,280 plants were visually assessed and 7,941 symptomatic plants were georeferenced.

The incidence of FW on the assessed fields in Brazil was moderate (mean = 10.7%) when compared to surveys performed in some regions in Africa (Mengesha et al. 2018; Karangwa et al. 2016). FW epidemics reach up to 77% of incidence in Southwest Ethiopia, with an average of 17.8% and a prevalence of 67% in plots (100 m^2) studied in 180 peasant farms (Mengesha et al. 2018). In East and Central Africa, disease incidence was greater than 40% in most of the fields

Preprints (www.preprints.org) | NOT PEER-REVIEWED | Posted: 15 July 2021 doi:10.20944/preprints202107.0352.v1

(Karangwa et al. 2016). Considering disease incidence, this study used a census to characterize the FW epidemics in the fields. The highest FW incidence was observed in NPP and SJA regions where there is a higher proportion of fields planted with the highly susceptible cultivar, Silk. Pome and Cavendish fields were significantly less affected by the disease, as these cultivars are moderately and highly resistant, respectively, to the *Foc* populations present in Brazil (Matos et al. 2009; Dita et al. 2018). However, this scenario might change if *Foc* TR4 surpasses the borders with Colombia (Garcia-Bastidas et al. 2019) and Peru (Peruvian National Service of Agricultural Safety 2021), or is introduced in Brazil by other ways.

In spite of occurring at moderate intensity, FW may have socio-economic impacts because many affected fields in the study are in low- or moderate-input farms, where the resource access to manage and reduce the disease impact are limited (Staver et al. 2020). Overall, at each 1% of FW incidence detected in the fields resulted in a loss of 184 Kg.ha.year. The median values of 11% of FW incidence with a median loss value of 935.2 $Kg.ha^{-1}.year^{-1}$, or US$ 405.10 $ha^{-1}.year^{-1}$ can substantially reduce the revenue from the crop. Bananas are cultivated in 468,000 hectares in Brazil (IBGE 2019). In a hypothetical scenario where 20% of the banana fields in Brazil are being affected by FW the estimated losses would be 87,534 ton and US$ 37.92 million yearly of the banana production in Brazil. Considering that Brazil has one of the highest per capita consumption (~60 Kg; FAO: http://www.fao.org/economic/est/est-commodities/bananas/bananafacts/en/#.YOnduejMPDc), the potential losses could feed 1.45 million people yearly. Unfortunately, some crucial information, such as local attainable yield and prices, and either the FW prevalence in Brazil, were not available for a precise estimation of the social-economic impact of the disease for farmers and consumers. Thus, the estimates may be used

Preprints (www.preprints.org) | NOT PEER-REVIEWED | Posted: 15 July 2021 doi:10.20944/preprints202107.0352.v1

as a baseline for farmers, industry and policymakers. Most likely, the real impact of FW in the banana industry is still underestimated.

Regarding the spatial distribution of FW, the aggregated pattern was detected in 43% of the fields by all spatial statistics and the random pattern was detected in 57% of the data sets by one or more analytical methods (Table 2). Some of the quadrat-based statistics (*D* and distribution fitting) resulted in a higher number of fields with an aggregated pattern compared to the distance-based methods (Table 2). The quadrat-based methods do not use the spatial information of the sampling units (Perry et al. 1999) and have limited capacity to describe the spatial pattern in the entire field. Inferences about heterogeneity are made at scales below the threshold at which the data were collected. However, these tests were important to detect the degree of heterogeneity within disease clusters when few clusters were present. When a quadrat-based method is used in association with distance-based methods the entire process of disease spread could be better studied. Notwithstanding, a clear relationship between quadrat and distance-based methods was not expected because of the intrinsic features adjusted for the different physical scales set to study spatial heterogeneity (Turechek and Madden 2001; Gigot et al. 2017).

Overall, FW had an aggregated pattern, but clusters of diseased plants (foci) were randomly distributed in the field. Thus, the way the initial inoculum is introduced in an area drives the spatial distribution of the disease of the epidemic. From a focus, neighboring plants are more likely to become infected originating the aggregated pattern. Consequently, a random pattern is likely to be detected at lower intensities, and aggregation may be detected after epidemics develop. These dynamics were revealed when analyzing the data with the binary power law: fields with lower incidences had weaker aggregation parameters than fields with higher incidence values observed in this study (Fig 5A). However, this fact was only observed because the highest incidence was

Preprints (www.preprints.org) | NOT PEER-REVIEWED | Posted: 15 July 2021 doi:10.20944/preprints202107.0352.v1

0.41. For foliar pathosystems where disease incidence above 50% is commonly observed, the binary power law's aggregation parameter is low in datasets with either very low or very high incidences (Gigot et al. 2017; Heck et al. 2021). Diseases caused by pathogens dispersed mostly from plant-to-plant usually present this pattern (Musoli et al., 2008; Rekah et al., 1999). Coffee wilt, caused by *Fusarium xylarioides*, and Fusarium crown and root rot of tomato, caused by *F. oxysporum* f. sp. *lycopersici* (*Fol*), illustrate this pattern of distribution (Musoli et al., 2008; Rekah et al., 1999). An aggregated pattern of FW was also found in Australia by the joint-count statistic (Meldrum et al., 2013). Apparently, wilted plants have a random pattern in the field at the beginning of the epidemics and changes to aggregation later on.

The random pattern of FW epidemics detected in some of the fields by one more spatial statistics may also warn about other processes affecting the dispersal of *Foc* to sites far from the main foci. Based on the semivariance analysis half of the fields had range values shorter than 30.8 m, meaning that the foci size on these fields are usually smaller than that. The range parameter is the maximum distance that the samples are spatially correlated (Chellemi et al. 1988). The spread of Fusarium crown and root rot in tomatoes ranged from 1.1 to 4.4 m (Rekah et al. 1999). Tomatoes are an annual crop with a short cycle and fields are normally cultivated at distances less than 50 cm within row. Bananas are a semi perennial crop cultivated at within row distances that range from 1.5 m to 7 m. In addition to plant-to-plant spread, weevil borer, other animals, cultural practices, wind, runoff or irrigation water may contribute to disease dissemination (Dita et al. 2018, Heck et al. 2021). Aerial dispersal of *Fol* and *F. oxysporum* f. sp. *cucumerinum* has been reported (Katan et al. 1997; Scarlett et al. 2015). Evidence of external sporulation of *Foc* in banana plants may suggest the potential role of wind and rain dispersion (Warman and Aitken 2018). It is hypothesized that feral pigs surrounding the fields (Biosecurity of Queensland 2016) and humans

 doi:10.20944/preprints202107.0352.v1

(Ploetz et al. 2015) are involved in the within and among field dispersal of *Foc* (Ploetz 2015; Dita et al. 2018). Insects as weevil borers can carry infective propagules of *Foc* (Sanchez et al. 2021) and their populations were driving FW epidemics in banana fields (Heck et al. 2021).

Many biological, cultural, and ecological processes can directly affect the spatial pattern of plant diseases (Campbell and Benson 1994). The study of the effect of cultivars in the distribution of FW indicated that the disease has an aggregated pattern and the level of aggregation varied with incidence. The power law parameter, log(*A*), was significantly different between Silk and Pome cultivars. Silk is more susceptible than Pome, thus a clearer aggregated pattern was more often observed in fields planted to the latter. Based on this pattern, it is possible to infer that FW can spread farther when epidemics occur in highly susceptible cultivars. Plants with intermediate resistance levels are less affected by FW up to certain densities of inoculum (Dita et al. 2018). In this way, the inoculum density - disease intensity (ID:DI) relationship may hold for FW as reported in other *F. oxysporum* pathosystems (Smith and Snyder 1971; Elmer 2002; Zhou and Everts 2003; Hao et al. 2009).

Soilborne pathogens give rise, in general, to monocyclic diseases (Vanderplank 1963). However, multiple cycles of infection may occur in banana plantations affected by *Foc* (Ploetz 2015; Pegg et al. 2019). The sigmoidal pattern observed for the plots of incidence over time suggests that multiple infections may have occurred in the FW epidemics along the two years of study. The semi-perennial nature of the banana plant and the impractical task of pathogen elimination from the soil means that once infected and infested by *Foc*, respectively, they may act as an inoculum source for an undetermined time. The intensive management to achieve high productivity and other mechanisms of dispersal during the growing season could affect the dynamics of the disease and were reported for other members of *F. oxysporum* (Rekah et al. 1999;

Preprints (www.preprints.org) | NOT PEER-REVIEWED | Posted: 15 July 2021 doi:10.20944/preprints202107.0352.v1

Scarlett et al. 2015, 2014). Similar argument was suggested for *Foc* in banana plantations (Meldrum et al. 2013; Heck et al. 2021). The field monitored was managed in a low-input system, so anthropogenic factors, such as cultural practices, were not performed before and during the study period. In this case, *Foc* dispersal is due to natural causes, such as root-to-root contact, vectors, floods or wind. A critical point of this result is that the highest incidence value observed for the FW epidemic was low (=0.15), and the full temporal dynamic of the epidemic (0 to 1) could not be completely characterized. Future studies addressing the temporal dynamic in different cultivars, pathogen populations, abiotic factors, and management practices can complement the epidemiological knowledge of the disease.

The spatio-temporal dynamics support the occurrence of secondary infection as indicated by the spatial and temporal analyses conducted separately. The ratio between the observed and expected variances (*D*) increased over time (Fig. 8A). However, the aggregation index (I_a) of a geospatial statistic (*SADIE*) remained unaltered (Fig. 8B). These facts showed a low level of aggregation, i.e. low number of diseased plants per sampling unit, at the beginning of the epidemic. Over time, the number of diseased individuals increased on the sampling units where diseased plants were already detected, increasing the ratio between the observed and expected variances, with no or little effect in the geospatial distribution of the foci. The observed pattern agrees with disease transmission to neighboring plants at a higher rate than to plants located farther apart in the field, mainly due to plant-to-plant spread. In addition, temporal associations of the local clustering indices indicated a strong evidence of correlations between the successive pairs of assessments. Only in the beginning of the epidemic, when the incidence was low, there was no association in some plots (Fig. 8D). However a lack of association between the first and the intermediate, and the first and the last assessment were observed (*data not shown*). Mechanisms

 doi:10.20944/preprints202107.0352.v1

of *Foc* dispersal to long distances (beyond the borders of the sampling unit) also affected the epidemics and were evidenced in the long term. This fact may be associated with disease spread beyond the borders of sampling units, by increase in foci size or spread to plants far from initial foci that could not be detected by others methods. Understanding how the inoculum arrives in the field and the mechanisms involved in *Foc* dispersal are key to propose efficient management strategies to reduce the impacts of FW epidemics.

In summary, the intensity of FW of bananas in Brazil was moderate (~11%) with losses up to 8.19 ton.ha^{-1}.year^{-1}. The disease distribution was predominantly aggregated with some fields presenting a random distribution of disease foci, which may be due to the way the initial inoculum was introduced and distributed. The polycyclic model best describes the initial development of the epidemic. After establishing the disease in the field, transmission to the neighboring plants seems to drive the epidemics in the short term, while the spatial distribution of foci are mainly affected by long-distance dispersal mechanisms. These insights about the epidemiology of FW can help banana farmers improve their decisions to manage the disease and reduce crop losses. Assuming the general pattern of non-TR4 populations of *Foc* could be used as a proxy, this large-scale study is also useful to policymakers in charge of formulation of actions to mitigate the consequences of the introduction of *Foc* TR4.

ACKNOWLEDGMENTS

This work was undertaken as part of the D.Sc. of the first author and the scholarship was supported by the National Council for Scientific and Technological Development - CNPq (Process 141026/2015-4). This study was financed in part by the Coordenação de Aperfeiçoamento de Pessoal de Nível Superior - Brasil (CAPES) - Finance Code 001. Funding support was also

provided by Brazilian Agricultural Research Corporation – Embrapa and The São Paulo Research Foundation – Fapesp. Special thanks to Dr. Francisco Laranjeira and Dr. Fernando Haddad (Embrapa, Brazil) for the critical reading of the manuscript.

REFERENCES

Alvarez, C. E., Garcia, V., Robles, J., and Diaz, A. 1981. Influence des caractéristiques du sol sur l´incidence de la Maladie de Panama. Fruits. 36:71–81.

Amir, H., and Alabouvette, C. 1993. Involvement of soil abiotic factors in the mechanisms of soil suppressiveness to Fusarium wilts. Soil Biol. Biochem. 25:157–164.

Baddeley, A., and Turner, R. 2005. Spatstat: an R package for analyzing spatial point patterns. J. Stat. Softw. 12:1–42.

Bancroft, J. 1876. Report of the board appointed to enquire into the cause of disease affecting livestock and plants. Votes and Proceedings 1877. 3:1011–1038.

Bataglia, O. C., Furlani, A. M. C., Teixeira, J. P. F., Furlani, P. R., and Gallo, J. R. 1983. *Métodos de análise química de plantas*. Campinas, SP, Brasil: Instituto Agronômico de Campinas.

Besag, J. 1977. Discussion of Dr Ripley's paper. J. R. Stat. Soc. B. 39:193–195.

Biosecurity of Queensland. 2016. *Panama disease tropical race 4: Biosecurity standards and guidelines*. 18p.

Camargo, O. A., Moniz, A. C., Jorge, J. A., and Valadares, J. M. A. S. 2009. *Métodos de análise química, mineralógica e física de solos do Instituto Agronômico de Campinas*. 2ª ed. Campinas, SP, Brasil: Instituto Agronômico de Campinas. 77p.

Campbell, C. L., and Benson, D. M. 1994. Spatial aspects of the development of root disease epidemics. In *Epidemiology and management of root diseases*, eds. C. L. Campbell and D. M.

Benson. Berlin, Heidelberg: Springer Berlin Heidelberg, p. 195–243.

Chellemi, D. O., Rohrbach, K. G., Yost, R. S., and Sonoda, R. M. 1988. Analysis of the Spatial Pattern of Plant Pathogens and Diseased Plants Using Geostatistics. Phytopathology. 78:221–226.

Deltour, P., França, S. C., Pereira, O. L., Cardoso, I., De Neve, S., Debode, J., et al. 2017. Disease suppressiveness to Fusarium wilt of banana in an agroforestry system: Influence of soil characteristics and plant community. Agric. Ecosyst. Environ. 239:173–181.

Dita, M., Barquero, M., Heck, D., Mizubuti, E. S. G., and Staver, C. P. 2018. Fusarium wilt of banana: Current knowledge on epidemiology and research needs toward sustainable disease management. Front. Plant Sci. 9:1468.

Dixon, P. M. 2002. Ripley's K function. In *Encyclopedia of environmetrics*, eds. Abdel H. El-Shaarawi and Walter W. Piegorsch. Chichester: John Wiley & Sons, p. 1796–1803.

Domínguez, J., Negrín, M. A., Rodríguez, C. M., Domínguez, J., Negrín, M. A., Rodríguez, C. M., et al. 2001. Aggregate water-stability, particle-size and soil solution properties in conducive and suppressive soils to Fusarium wilt of banana from Canary Islands (Spain). Soil Biol. Biochem. 33:449–455.

Elmer, W. H. 2002. Influence of inoculum density of Fusarium oxysporum f. sp. cyclaminis and sodium chloride on cyclamen and the development of Fusarium wilt. Plant Dis. 86:389-393.

Gamer, M., Lemon, J., Fellows, I., and Singh, P. 2012. *IRR: Various coefficients of interrater reliability and agreement*. CRAN. Available at: http://www.r-project.org.

García-Bastidas, F. A., Quintero-Vargas, J. C., Ayala-Vasquez, M., Schermer, T., Seidl, M. F., Santos-Paiva, M., Noguera, A. M., Aguilera-Galvez, C., Wittenberg, A., Hofstede, R. and Sørensen, A. 2020. First report of Fusarium wilt Tropical Race 4 in Cavendish bananas caused by Fusarium odoratissimum in Colombia. Plant Dis. 104:994-994.

 doi:10.20944/preprints202107.0352.v1

Gigot, C. 2018. *Epiphy: Analysis of plant disease epidemics*. CRAN. Available at: https://github.com/chgigot/epiphy.

Gigot, C., Turechek, W. W., and McRoberts, N. 2017. Analysis of the spatial pattern of strawberry angular leaf spot in California nursery production. Phytopathology. 107:1243–1255.

Haddad, F., Rocha, L. S., Soares, A. C. F., Martins, I. P. S., Teixeira, L. A. J., Staver, C., et al. 2018. Management of Fusarium wilt of bananas in Minas Gerais, Brazil. Acta Hortic. 1196:137–146.

Hao, J. J., Yang, M. E., and Davis, R. M. 2009. Effect of soil inoculum density of *Fusarium oxysporum* f. sp. *vasinfectum* race 4 on disease development in cotton. Plant Dis. 93:1324-1328.

Heck, D.W., Alves, G. and Mizubuti, E.S., 2021. Weevil borers affect the spatio-temporal dynamics of banana Fusarium wilt. J. Fungi. 7:329.

Horne, J. K., and Schneider, D. C. 1995. Spatial variance in ecology. Oikos. 74:18–26.

Hughes, G., and Gottwald, T. R. 1999. Survey methods for assessment of citrus tristeza virus incidence when *Toxoptera citricida* is the predominant vector. Phytopathology. 89:487–494.

Husson, F., Josse, J., Le, S., and Mazet, J. 2018. *FactoMineR: Multivariate exploratory data analysis and data mining*. CRAN. Available at: http://factominer.free.fr.

IBGE. 2019. Levantamento sistemático da produção agrícola. Available at: https://sidra.ibge.gov.br/tabela/1618.

Jerez, F. G., Castillo, I. T. J. del, and Perez, A. B. 1983. Estudio sobre el mal de Panama en las Islas Canarias: Caracteristicas físicas y quimicas de los suelos y su relacion con la aparición de la enfermedad. Fruits. 38:677–682.

Jones, C. A. 1983. Effect of soil texture on critical bulk densities for root growth. Soil Sci. Soc. Am. J. 47:1208.

 doi:10.20944/preprints202107.0352.v1

Karangwa, P., Blomme, G., Beed, F., Niyongere, C., and Viljoen, A. 2016. The distribution and incidence of banana Fusarium wilt in subsistence farming systems in east and central Africa. Crop Prot. 84:132–140.

Katan, T., Shlevin, E., and Katan, J. 1997. Sporulation of *Fusarium oxysporum* f. sp. *lycopersici* on stem surfaces of tomato plants and aerial dissemination of inoculum. Phytopathology. 87:712–719.

Leslie, J. F., and Summerell, B. A. 2008. *The Fusarium Laboratory Manual*. John Wiley & Sons.

Li, B., Madden, L. V., and Xu, X. 2012. Spatial analysis by distance indices: An alternative local clustering index for studying spatial patterns. Methods Ecol. Evol. 3:368–377.

Liu, L., Liang, C. C., Zeng, D., Yang, L. Y., Qin, H. Y., Wang, G. F., et al. 2015. Spatial distribution pattern for the Fusarium wilt disease in banana field and the *Fusarium oxysporum* f. sp. *cubense* in different parts of banana plants. Acta Ecol. Sin. 35:4742–4753.

Macedo, M. A., Inoue-Nagata, A. K., Silva, T. N. Z., Freitas, D. M. S., Rezende, J. A. M., Barbosa, J. C., et al. 2019. Temporal and spatial progress of the diseases caused by the crinivirus tomato chlorosis virus and the begomovirus tomato severe rugose virus in tomatoes in Brazil. Plant Pathol. 68:72–84.

Madden, L. V. 1989. Dynamic nature of within-field disease and pathogen distributions. In *Spatial components of plant disease epidemics*, ed. M. J. Jeger. Englewood Cliffs, NJ: Prentice-Hall, p. 96–126.

Madden, L. V., and Hughes, G. 1995. Plant disease incidence: Distributions, heterogeneity, and temporal analysis. Annu. Rev. Phytopathol. 33:529–564.

Madden, L. V., and Hughes, G. 1999. Sampling for plant disease incidence. Phytopathology. 89:1088–1103.

Madden, L. V., Hughes, G., and Bosch, F. 2007. *The study of plant disease epidemics*. MN, USA: American Phytopathological Society (APS Press).

Madden, L. V., Hughes, G., and Munkvold, G. P. 1996. Plant disease incidence: inverse sampling, sequential sampling, and confidence intervals when observed mean incidence is zero. Crop Prot. 15:621–632.

Meldrum, R. A., Daly, A. M., Tran-Nguyen, L. T. T., and Aitken, E. A. B. 2013. Are banana weevil borers a vector in spreading *Fusarium oxysporum* f. sp. *cubense* tropical race 4 in banana plantations? Australas. Plant Pathol. 42:543–549.

Mengesha, G. G., Yetayew, H. T., and Sako, A. K. 2018. Spatial distribution and association of banana (*Musa* spp.) Fusarium wilt (*Fusarium oxysporum* f. sp. *cubense*) epidemics with biophysical factors in southwestern Ethiopia. Arc. Phytopath. Plant Prot. 0:1–26.

Musoli, C. P., Pinard, F., Charrier, A., Kangire, A., Ten Hoopen, G. M., Kabole, C., et al. 2008. Spatial and temporal analysis of coffee wilt disease caused by *Fusarium xylarioides* in *Coffea canephora*. Eur. J. Plant Pathol. 122:451–460.

Orr, R., and Nelson, P. N. 2018. Impacts of soil abiotic attributes on Fusarium wilt, focusing on bananas. Appl. Soil Ecol. 132:20–33.

Perry, J. N., Winder, L., Holland, J. M., and Alston, R. D. 1999. Red-blue plots for detecting clusters in count data. Ecol. Lett. 2:106–113.

Peruvian National Service of Agricultural Safety Agrarian Health Service. 2021. SENASA confirma brote de Fusarium Raza 4 Tropical en Piura. Servicio Nacional de Sanidad Agraria del Perú. Available at: https://www.gob.pe/institucion/senasa/noticias/429832-senasa-confirma-brote-de-fusarium-raza-4-tropical-en-piura. Accessed on: 25 June 2021.

 doi:10.20944/preprints202107.0352.v1

Ploetz, R. C. 2006. Fusarium wilt of banana is caused by several pathogens referred to as Fusarium oxysporum f. sp. cubense. Phytopathology. 96:653-656.

Ploetz, R. C. 2015. Fusarium wilt of banana. Phytopathology. 105:1512–1521.

Ploetz, R., Freeman, S., Konkol, J., Al-Abed, A., Naser, Z., Shalan, K., et al. 2015. Tropical race 4 of Panama disease in the Middle East. Phytoparasitica. :283–293.

Raij, B. V., Andrade, J. C., Cantarella, H., and Quaggio, J. A. 2001. *Análise química para avaliação da fertilidade de solos tropicais*. Campinas, SP: Instituto Agronômico de Campinas.

Rekah, Y., Shtienberg, D., and Katan, J. 1999. Spatial distribution and temporal development of Fusarium crown and root rot of tomato and pathogen dissemination in field soil. Phytopathology. 89:831–839.

Ribeiro, P. J., Jr, and Diggle, P. J. 2018. *geoR: analysis of geostatistical data*. CRAN. Available at: https://cran.r-project.org/package=geoR.

Rishbeth, J. 1957. Fusarium wilt of bananas in Jamaica. Ann. Bot. 21:215–245.

Ristaino, J. B., and Gumpertz, M. L. 2000. New frontiers in the study of dispersal and spatial analysis of epidemics caused by species in the genus *Phytophthora*. Annu. Rev. Phytopathol. 38:541–576.

Guillen Sanchez, C., Tixier, P., Tapia Fernandez, A., Conejo Barboza, A.M., Sandoval Fernández, J.A. and De Lapeyre de Bellaire, L., 2021. Can the banana weevil *Cosmopolites sordidus* be a vector of *Fusarium oxysporum* f. sp. *cubense* race 1? Unravelling the internal and external acquisition of effective inoculum. Pest Manag. Sci. 77:3002-3012.

Scarlett, K., Tesoriero, L., Daniel, R., Maffi, D., Faoro, F., and Guest, D. I. 2015. Airborne inoculum of *Fusarium oxysporum* f. sp. *cucumerinum*. Eur. J. Plant Pathol. 141:779–787.

 doi:10.20944/preprints202107.0352.v1

Smith, S. N., and Snyder, W. C. 1971. Relationship of inoculum density and soil type to severity of Fusarium wilt of sweet potato. Phytopathology. 61:1049-1051.

Snyder, W. C., and Hansen, H. N. 1940. The species concept in *Fusarium*. Am. J. Bot. 27:64.

Stover, R. H. 1962. Fusarial wilt (Panama Disease) of bananas and other *Musa* species. In *Phytopathol. Pap.*, ed. R. H. Stover. Kew, Surrey, England: Commonw. Mycol. Inst., p. 117.

Szmyt, J. 2014. Spatial statistics in ecological analysis: from indices to functions. Silva Fenn. 48:31 p.

Torres-Bedoya, E., Bebber, D. and Studholme, D. J. 2021. Taxonomic revision of the banana Fusarium wilt TR4 pathogen is premature. Phytopathology. https://doi.org/10.1094/PHYTO-03-21-0089-LE.

Turechek, W. W. and Madden, L. V., 2001. Effect of scale on plant disease incidence and heterogeneity in a spatial hierarchy. Ecol. Modell. 144:77-95.

Turechek, W. W., and McRoberts, N. 2013. Considerations of scale in the analysis of spatial pattern of plant disease epidemics. Annu. Rev. Phytopathol. 51:453–472.

Warman, N. M., and Aitken, E. A. B. 2018. The movement of *Fusarium oxysporum* f. sp. *cubense* (sub-tropical race 4) in susceptible cultivars of banana. Front. Plant Sci. 9:1748.

Zhou, X. G., and Everts, K. L. 2003. Races and inoculum density of *Fusarium oxysporum* f. sp. *niveum* in commercial watermelon fields in Maryland and Delaware. Plant Dis. 87:692-698.

Preprints (www.preprints.org) | NOT PEER-REVIEWED | Posted: 15 July 2021 doi:10.20944/preprints202107.0352.v1

Table 1. Characteristics of fields assessed for Fusarium wilt of banana in Brazil.

Field ID	Municipality, state	Region[a]	Cultivar subgroup (genotype)	Area (ha)	Incidence ($\hat{p}$)
1	São Bento do Sapucaí, SP	SMZM	Pome (AAB)	2.82	1.66
2	São Bento do Sapucaí, SP	SMZM	Pome (AAB)	2.57	17.66
3	São Bento do Sapucaí, SP	SMZM	Pome (AAB)	2.08	4.82
4	São Bento do Sapucaí, SP	SMZM	Pome (AAB)	0.85	25.82
5	São Bento do Sapucaí, SP	SMZM	Pome (AAB)	1.29	7.92
6	Adolfo, SP	SJA	Silk (AAB)	6.67	41.42
7	Barbosa, SP	SJA	Silk (AAB)	3.86	4.94
8	Barbosa, SP	SJA	Silk (AAB)	3.33	36.9
9	Santa Mariana, PR	NPP	Silk (AAB)	6.40	11.49
10	Santa Mariana, PR	NPP	Silk (AAB)	2.23	32.77
11	Marinópolis, SP	SJA	Silk (AAB)	3.17	6.77
12	Marinópolis, SP	SJA	Silk (AAB)	2.78	12.39
13	Marinópolis, SP	SJA	Silk (AAB)	0.95	16.14
14	Palmeira d'Oeste, SP	SJA	Silk (AAB)	4.33	3.99
15	Marinópolis, SP	SJA	Silk (AAB)	0.99	19.42
16	Jacupiranga, SP	VR	Cavendish (AAA)	1.64	2.74
17	Jacupiranga, SP	VR	Pome (AAB)	2.43	10.42
18	Eldorado, SP	VR	Pome (AAB)	1.38	5.03
19	Jacupiranga, SP	VR	Pome (AAB)	1.35	3.26
20	Serra do Ramalho, BA	NMSF	Pome (AAB)	3.50	3.34
21	Janaúba, MG	NMSF	Pome (AAB)	5.94	0.09

Preprints (www.preprints.org) | NOT PEER-REVIEWED | Posted: 15 July 2021 doi:10.20944/preprints202107.0352.v1

22	Janaúba, MG	NMSF	Pome (AAB)	3.55	0.49
23	Jaíba, MG	NMSF	Pome (AAB)	2.34	4.44
24	Jaíba, MG	NMSF	Pome (AAB)	6.19	5.31
25	Corupá, SC	NC	Pome (AAB)	5.50	0.48
26	Corupá, SC	NC	Cavendish (AAA)	3.92	2.81
27	Corupá, SC	NC	Cavendish (AAA)	2.93	1.75
28	Corupá, SC	NC	Pome (AAB)	2.24	1.66
29	Corupá, SC	NC	Pome (AAB)	2.64	33.37
30	Teixeiras, MG	SMZM	Pome (AAB)	4.80	1.03

[a] SMZM - Serra da Mantiqueira and Zona da Mata; SJA - São José do Rio Preto and Araçatuba; NPP - Norte Pioneiro Paranaense; VR - Vale do Ribeira; NMSF - Norte de Minas and Vale do São Francisco da Bahia; NC - Norte Catarinense.

Preprints (www.preprints.org) | NOT PEER-REVIEWED | Posted: 15 July 2021 doi:10.20944/preprints202107.0352.v1

Table 2. Percentage of fields with significant aggregation by the index of dispersion (*D*), *β*-binomial parameter (θ), log-likelihood ratio statistic (LRS), index of aggregation of the *Spatial Analysis by Distance IndicEs* procedure (I_a), events and intervals ($D_{K\text{-}S}$), and linear transformation of Ripley's K function ($L(d)$ function) to each region assessed for incidence of Fusarium wilt of banana in Brazil [a].

Region [b]	*D* [c]	θ [c]	LRS [c]	I_a [c]	$D_{K\text{-}S}$ [d]	$L(d)$ function [d]
SMZM (n = 6)	100	100	100	66.7	100	100
SJA (n = 8)	100	75	100	37.5	50	100
NPP (n = 2)	100	100	100	50	100	100
VR (n = 4)	100	100	100	100	100	100
NMSF (n = 5)	80	80	80	80	80	80
NC (n = 5)	100	100	100	80	40	100
Overall (n = 30)	96.7	90	96.7	66.7	73.3	96.7

[a] The aggregated pattern was inferred when the null hypothesis of randomness was rejected ($P < 0.05$). The null hypothesis of the *β*-binomial parameter (θ) is aggregation ($P > 0.05$).

[b] SMZM - Serra da Mantiqueira and Zona da Mata; SJA - São José do Rio Preto and Araçatuba; NPP - Norte Pioneiro Paranaense; VR - Vale do Ribeira; NMSF - Norte de Minas and Vale do São Francisco da Bahia; NC - Norte Catarinense.

[c] Quadrat-based statistics with quadrat-size of 3 x 3 plants.

[d] Distance-based statistic.

Preprints (www.preprints.org) | NOT PEER-REVIEWED | Posted: 15 July 2021 doi:10.20944/preprints202107.0352.v1

Table 3. Cohen's and Fleiss's Kappa agreement and proportions of fields with the same classification for index of aggregation (*D*), *β*-binomial distribution, Spatial Analysis by Distance IndicEs (I_a), events and intervals ($D_{K\text{-}S}$) and Maximum Absolute Deviation (MAD) statistic from $L(d)$ function for 30 fields assessed for Fusarium wilt incidence in Brazil [a].

Spatial statistic [b]	θ	I_a	$D_{K\text{-}S}$	MAD
D	-0.05 (26/30)	-0.06 (19/30)	-0.06 (21/30)	**1.00** (30/30)
θ		-0.18 (17/30)	-0.17 (19/30)	-0.05 (26/30)
I_a			**0.37** (22/30)	-0.06 (19/30)
$D_{K\text{-}S}$				-0.06 (21/30)
Overall [c]	-0.027 (13/30)			

[a] The pattern of FW in the fields was classified as aggregated or random according to the spatial statistics. Kappa values in bold differed significantly from 0 (random classification) by z statistic ($P < 0.05$). The proportion of fields classified in the same spatial pattern of FW is shown in parentheses.

[b] Cohen's Kappa paired agreement between tests.

[c] Fleiss's Kappa overall agreement among the tests.

Preprints (www.preprints.org) | NOT PEER-REVIEWED | Posted: 15 July 2021 doi:10.20944/preprints202107.0352.v1

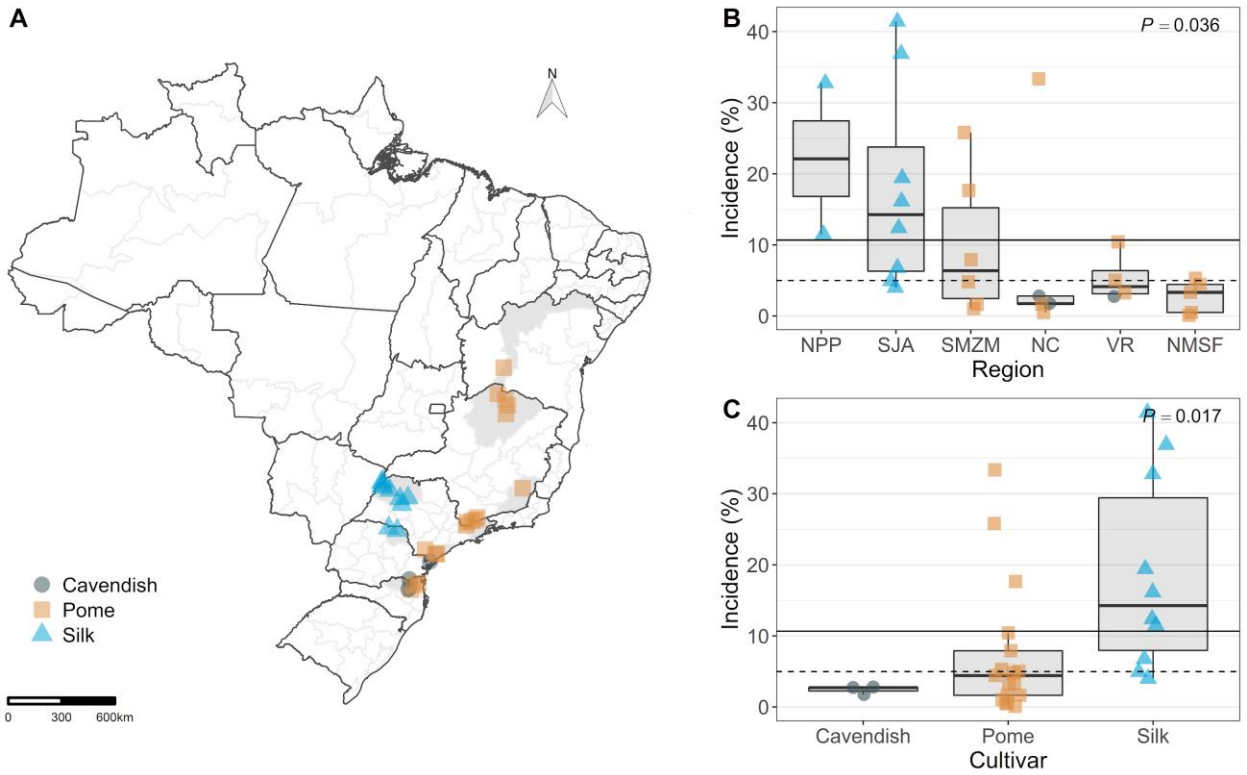

Fig. 1. A) Location of the 30 sampled fields distributed in five states of Brazil. Meso-regions are shaded in gray and the exact location of the fields was identified by geometrical shapes that correspond to banana cultivars. Fields located close to each other appear superimposed on the map and geometric shapes are darker. B) Boxplots for incidence of Fusarium wilt on banana fields in different regions from Brazil and C) for different cultivars. The overall mean and median values are represented by dashed and solid lines, respectively. P-values from the analysis of variance for unbalanced data.

Preprints (www.preprints.org) | NOT PEER-REVIEWED | Posted: 15 July 2021 doi:10.20944/preprints202107.0352.v1

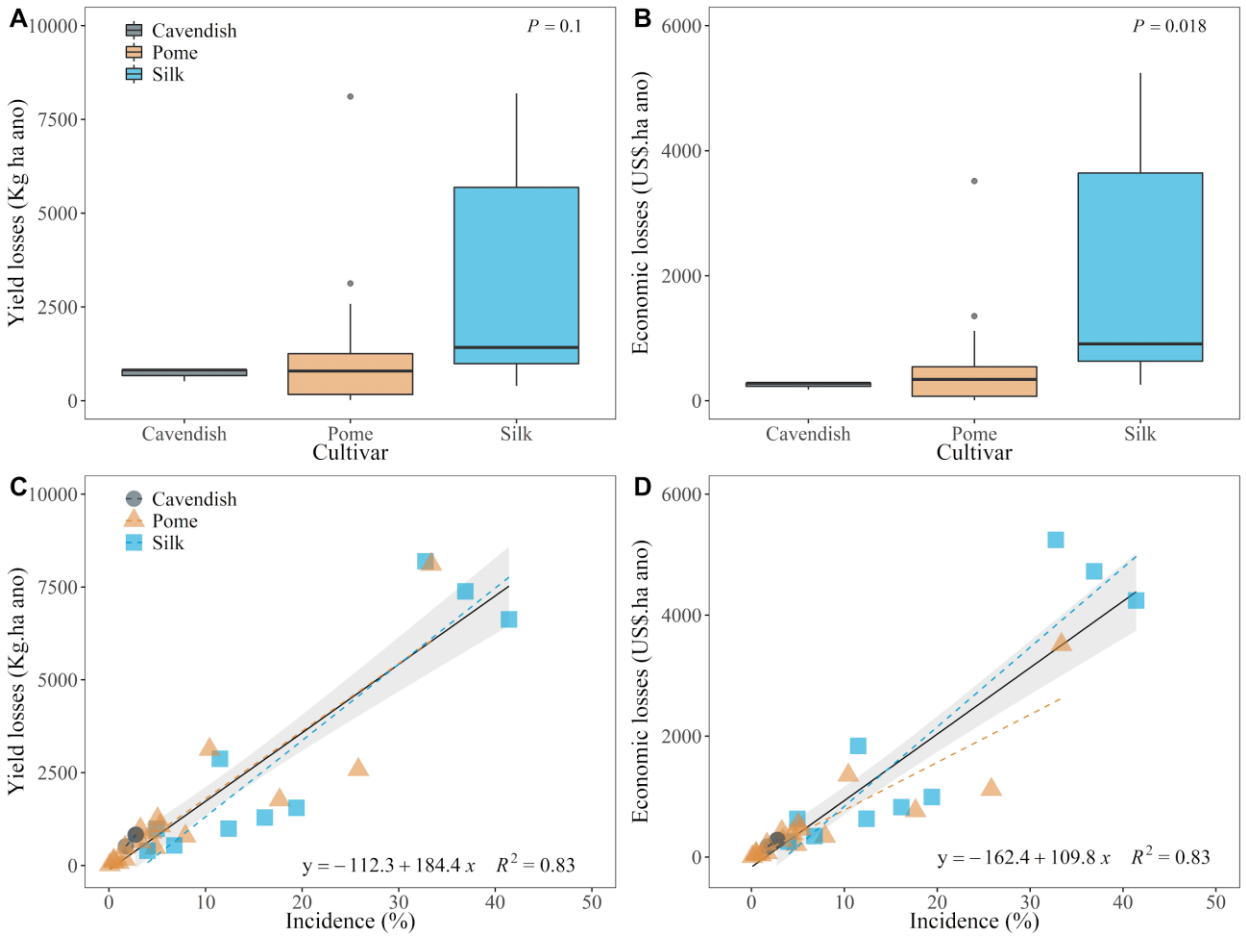

Fig. 2. Estimated values of yield and economic losses and its relationship with incidence of Fusarium wilt of banana assessed in 30 fields from different cultivars and regions of Brazil. A) Frequency of estimated values of yield losses, and B) economic losses. C) Estimated values (dots) for each assessed field and overall regression (solid black) and cultivar regression lines (dashed colored) for the relationship between yield losses, and D) economic losses. P-values in A and B, and regression equations in C and D are presented in figures. Confidence intervals (CI95%) are presented in C and D as shaded areas.

Preprints (www.preprints.org) | NOT PEER-REVIEWED | Posted: 15 July 2021 doi:10.20944/preprints202107.0352.v1

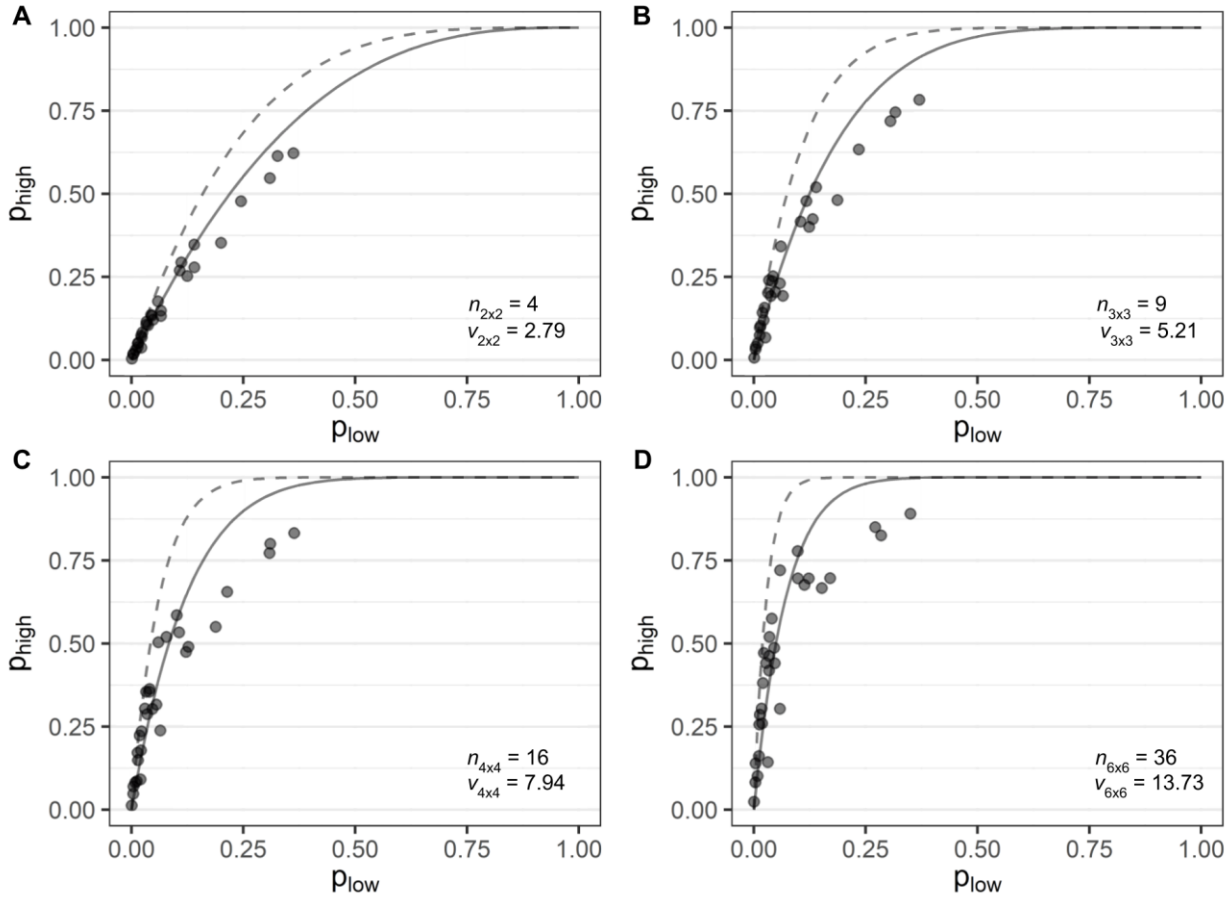

Fig. 3. Relationships between the incidence of Fusarium wilt of banana at A) 2 x 2; B) 3 x 3; C) 4 x 4; and D) 6 x 6 quadrat dimensions in 30 banana fields. The sampling unit (quadrat) was the highest (p_{high}) hierarchical level and the individual (plants) was the lowest (p_{low}). Binomial (dashed-lines) and β-binomial (solid-lines) distributions were fit to the data. The number of individuals (n) and the effective sample size (v) estimated at each level are presented in the graphs.

Preprints (www.preprints.org) | NOT PEER-REVIEWED | Posted: 15 July 2021 doi:10.20944/preprints202107.0352.v1

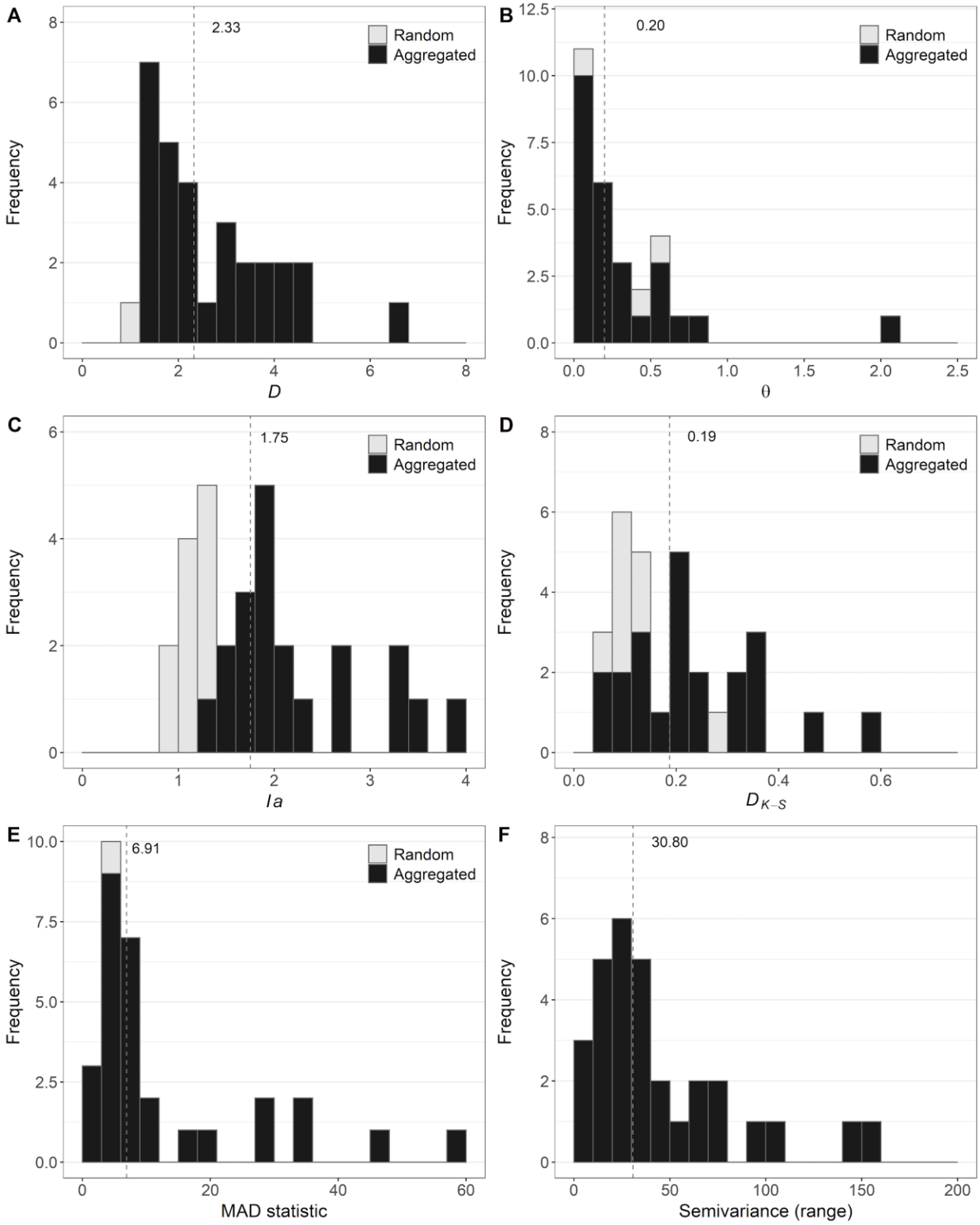

Fig 4. Histograms of A) the index of dispersion (D), B) β-binomial parameter (θ) from distribution fitting, C) aggregation index (I_a) from *Spatial Analysis by Distance IndicEs* (*SADIE*), D) events

Preprints (www.preprints.org) | NOT PEER-REVIEWED | Posted: 15 July 2021 doi:10.20944/preprints202107.0352.v1

and intervals ($D_{K\text{-}S}$), E) Maximum Absolute Deviation (MAD) statistic from $L(d)$ function, and F) range from semivariance analyses of Fusarium wilt of banana? The frequencies were based on 30 fields assessed for incidence of Fusarium wilt of banana in Brazil. Median value of the corresponding statistic is presented numerically on the graphs (dashed line). The classification of fields is represented as random (gray) or aggregated (black).

Preprints (www.preprints.org) | NOT PEER-REVIEWED | Posted: 15 July 2021 doi:10.20944/preprints202107.0352.v1

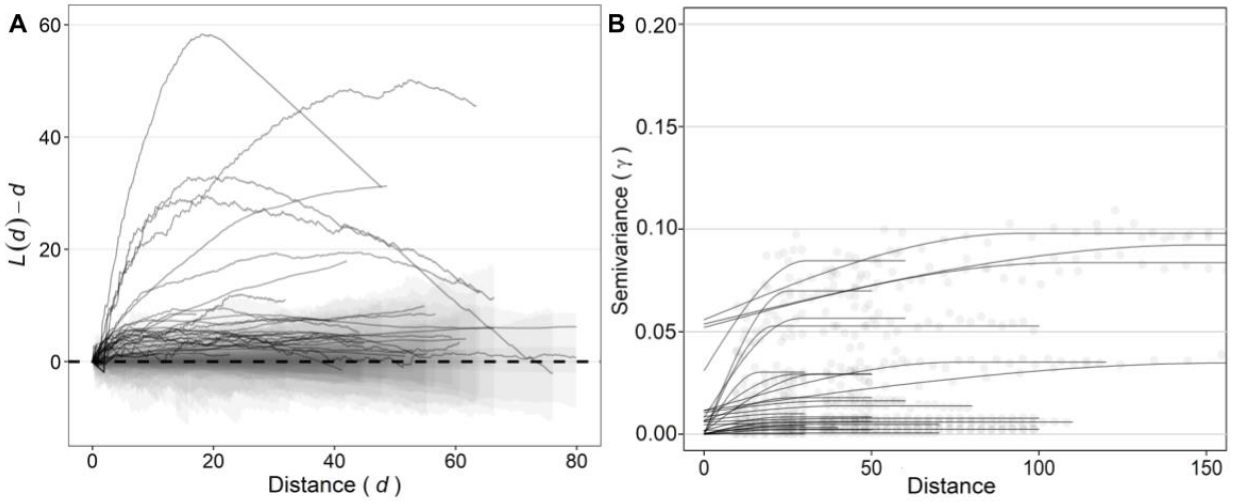

Fig. 5. Distance-based statistics of the incidence of Fusarium wilt of banana in 30 fields in Brazil. A) L(d) - d against d (solid line), superimposed envelopes (shaded area) and the random pattern (dashed line) are presented. B) Semivariance (γ) in a range of distances was represented by spherical model fitted to the data. Fields were represented by solid lines. Distances are presented in meters (m).

Preprints (www.preprints.org) | NOT PEER-REVIEWED | Posted: 15 July 2021 doi:10.20944/preprints202107.0352.v1

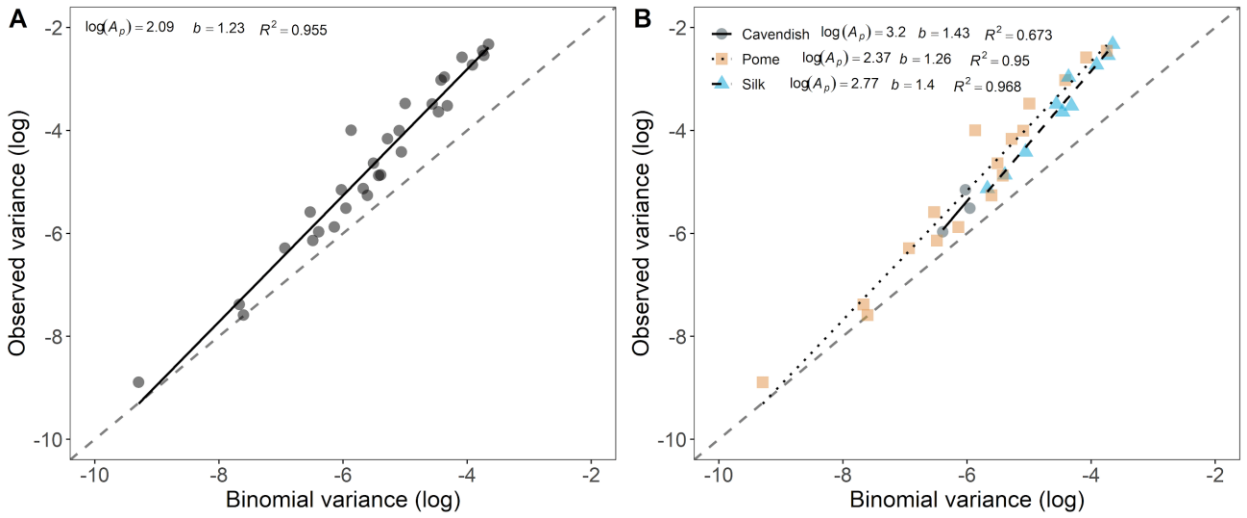

Fig 6. Relationship between the logarithm of the observed variance ($\log(s^2)$) and the logarithm of theoretical variance ($\log(s^2_{bin})$) for incidence data of Fusarium wilt of banana in 30 fields in Brazil. A) Linear regression for all 30 fields assessed for disease incidence (solid dark line), and B) for Silk (n = 10 fields), Cavendish (n = 3) or Prata (n = 17) cultivars. Binomial lines are represented by solid gray lines. Binary power law parameters ($\log(A_p)$ and b) were presented

Preprints (www.preprints.org) | NOT PEER-REVIEWED | Posted: 15 July 2021 doi:10.20944/preprints202107.0352.v1

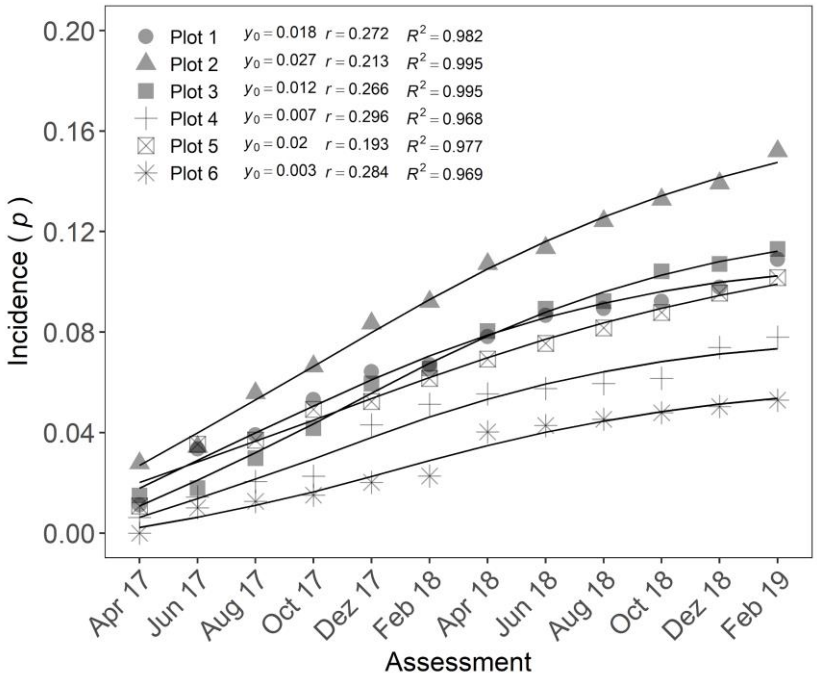

Fig. 7. Gompertz model adjusted to incidence data of Fusarium wilt of banana from April 2017 to February 2019 in six plots located in Teixeiras, Minas Gerais, Brazil. Dots referred to observed incidence in proportion (*p*) and solid lines for the predicted incidence by Gompertz model.

Preprints (www.preprints.org) | NOT PEER-REVIEWED | Posted: 15 July 2021 doi:10.20944/preprints202107.0352.v1

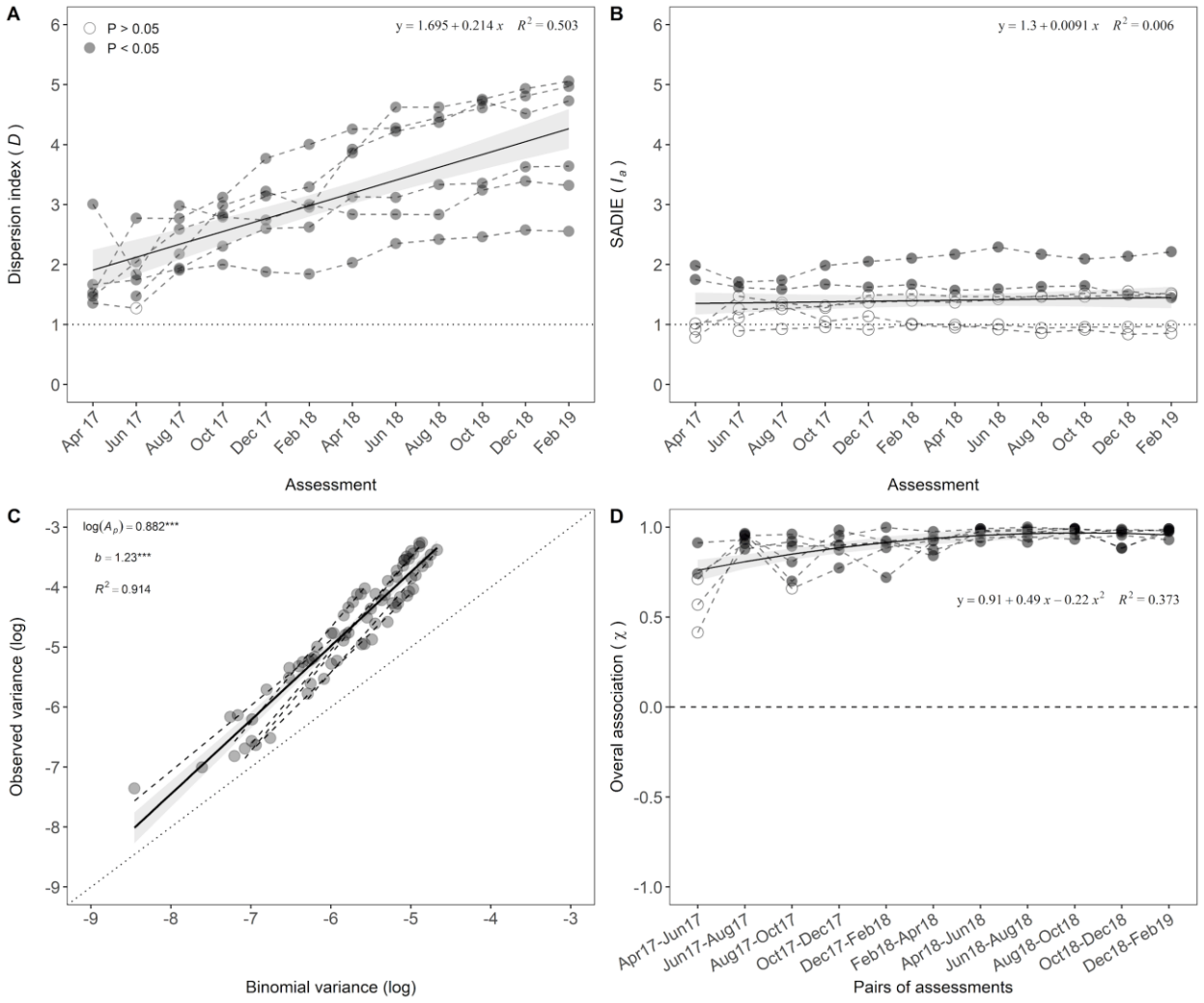

Fig 8. Spatio-temporal statistics used to characterize the dynamics of Fusarium wilt of banana in six plots assessed in Teixeiras, Minas Gerais, Brazil, from April 2017 to February 2019. A) Fisher's aggregation index (*D*), B) Spatial Analysis by Distance IndicEs (*SADIE*; I_a), C) binary power law, and D) spatio-temporal association of successive assessments of clustering indices. Open and closed dots were presented when the null hypothesis of randomness was not rejected ($P > 0.05$) or rejected ($P < 0.05$), respectively. Average statistic for all plots (solid line) and confidence interval (CI95%; shaded area) are presented. Equation or summary statistics were presented when applicable.

 doi:10.20944/preprints202107.0352.v1